Proceedings of the 21st ICSMGE, Vienna, Austria, 14 – 19 June 2026. Pistrol, Adam & Schweiger (eds.)
Published by: ÖGG, Austrian Society for Geomechanics, Salzburg, Austria, ISBN 978-3-9503898-4-5
https://doi.org/10.53243/ICSMGE2026-878

Construction Technology and Bearing Characteristics of Rock Socketed Piles Using in Yantian Port

Liwen Hu[1, 2], Qiongyu Wang[1, 2]
1. CCCC Fourth Harbor Engineering Institute Co., Ltd., Guangzhou 510230, China,1174624752@qq.com
2. Guangzhou Harbor Engineering Quality Exzamination Co. Ltd., Guangzhou 510230, China

Zhenhua Hu
The Second Engineering Company of CCCC Fourth Harbor Engineering Co., Ltd., Guangzhou 510230, China

Jian Liu
College of Civil and Transportation Engineering, Hohai University, Nanjing 210098, China

ABSTRACT: The side friction resistance parameters of the cast-in-place piles in the moderately weathered granite rock were not provided in the geotechnical investigation report of the Yantian Port project. To obtain this parameter and effectively guide the design of the pile length for this project, relying on the Yantian Port project, a construction technology of the offshore rock socketed piles which are composed of steel pipe pile and cast-in-place pile has been proposed and applied succesfully, and the bearing characteristics of rock socketed piles were studied using self-balancing tests. The mechanism of the side friction resistance of the piles under different loads was revealed. The results showed that For granite formations, when the penetration is not less than 30 mm/stroke, the toe of the steel pile does not crimp during driving. The side friction resistance per unit area of cast-in-place pile at moderately weathered granite is discoved as not less than 509.36 kPa, and the tensile side friction coefficient （or side friction coefficient of secondary type compression）is about 0.9. The theoretical value of the ultimate axial compressive bearing capacity of the test pile is determined and can be used to guide the design and construction of the rock socketed piles which are composed of steel pipe pile and cast-in-place pile in environments with severe wind and wave currents.

KEYWORDS: Pile foundation, rock socketed piles, bearing characteristics, self-balancing test, side friction coefficient.

1 INTRODUCTION

Yantian Port, as one of the benchmarks for container port construction in China, is an important gateway for China's trade and export. The construction of Yantian Port began as early as the 1990s. The foundation of this port is commonly composed of steel pipe pile and cast-in-place pile and anchored piles. Yantian Port has accumulated the construction technology of rock socketed piles (Chen, 1999), and the technical parameters of anchors within the piles (Hu, 2006). In 2023, considering the similar geological codition of shallow-buried rock formation and the applicability of rock socked piles in Yantian harbor area,the same type of pile has still been adopted as the foundation for the East harbor Phase I project. The rock socked pile consists of two parts: the upper permanent steel pipe pile with inner cast-in-place reinforced pile, and the bottom cast-in-place reinforced pile. For the construction of driving steel pipe pile in shallow buried or exposed granite where the wind and wave currents are worse, due to the insufficient depth of the steel pipe piles into the rock, how to stabilize the steel pipe piles after they are driven into the ground to ensure that the piles do not shift or even topple under the impact of the waves is one of the main difficulties in this project.

For shallow-buried rock layers as the bearing stratum of the piles, their bearing characteristics are particularly crucial. Some literature revealed that when conducting static load tests in different rock layers, shaft friction tests were carried out simultaneously (Lou et al., 2018; Xue et al, 2022; Zhang et al., 2023; Wu et al, 2021; Wu et al, 2022; Xu et al, 2012; Han & Qian, 2023). Due to the lack of unit area side resistance and end resistance of the bearing rock layer (i.e., moderately weathered granite) in the geological survey data of this project, there were difficulties in determining the depth of the cast-in-place pile into the rock. To obtain these parameters, based on the self-balancing test method (Hu et al., 2023), the stress sensors for shaft friction tests are instrumented, which can more accurately analyze their bearing characteristics.

Based on the resutlts of the self-balancing test and shaft friction test of a rock socketed pile which is composed of steel pipe pile and cast-in-place pile in the shallow-buried area of the Phase I Project of the East Port Area of Yantian Port, this paper studies the bearing characteristics of the rock socketed pile, and presents the construction technology of the offshore rock socketed piles in shallow-buried rock strata, as well as the values of the side friction resistance and end resistance of cast-in-place piles in moderately weathered granite, which provide a reference for similar geological ports and other engineering projects.

2 ENGINEERING AND GEOLOGICAL OVERVIEW

The Phase I Project of the East Port Area of Yantian Port consists of three 200,000-ton container berths, with a total shoreline length of 1,470 m. The wharf adopts the piles which are composed of steel pipe pile and cast-in-place pile as the structural foundation. The concrete strength grade of the pile body is C40. There are two types of piles under the track beam: straight piles and inclined piles.

After dredging, from the shore side towards the sea side, the thickness of covering layers of soil decreases significantly, even the piles closest to the sea side are in bare rock layers. That is, the soil cover layer above the rock layer in the shore side area is thicker, while the soil cover layer in the sea side area is thinner. The bearing stratum in the shallow-buried rock layer area is moderately weathered granite. According to different regions and different requirements for bearing capacity, the design requires that the pile toe penetrates the moderately weathered granite at a depth of 5 m and 10 m. Taking the A3-21# test pile as an example, this pile is located in the shallow-buried rock layer, and its information is shown in Table 1. The distribution of the nearby strata is shown in Figure 1, and the recommended values of the corresponding foundation design parameters are shown in Table 2.

Table 1. Test pile information

Pile name (#)	Pile diameter (mm)	Wall Thickness (mm)	Level of ground (m)	Level of pile top (m)	Bottom level of steel pipe section (m)	Bottom level of concrete section (m)
A3-21	1000	18	-12.67	+3.95	-18.36	-26.17

Table 2. Recommended values for foundation design parameters

Soil layer number and name	SPT N	Precast pile		Cast-in-place pile	
		Standard values of the ultimate frictional resistance at the pile side q_f (kPa)	Standard values of the ultimate resistance at the pile toe q_R (kPa)	Standard values of the ultimate frictional resistance at the pile side q_f (kPa)	Standard values of the ultimate resistance at the pile toe q_R (kPa)
③$_2$ Silty clay	7~16	15~45	/	10~40	/
③$_{2-1}$ Silty clay	4~7	35~45	/	30~35	/
⑤ Granite residual soil	15~33	70	/	55	/
○, 9$_{2-2}$ Fragmented, strongly weathered granite	>>50	250	10000	200	2500
○, 9$_3$ Moderately weathered granite	/	/	/	/	12000

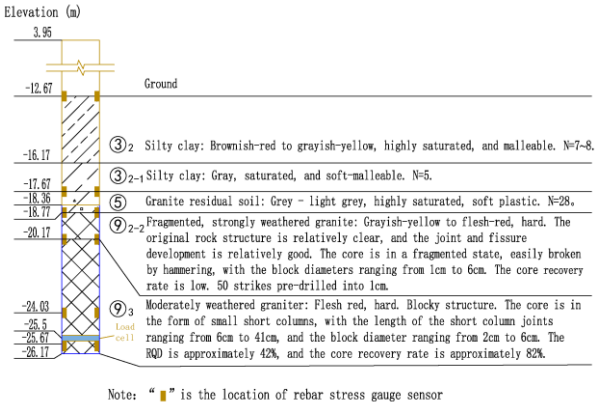

Figure 1. Soil distribution and location of rebar stress gauge sensor of test pile.

3 CONSTRUCTION TECHNOLOGY AND TEST OVERVIEW

3.1 *Construction Technology*

For the pile driving of this project, two types of pile-driving vessels, namely the "Yuegong 08" and the "Yuehang 03", were used. The pile frame of the "Yuegong 08" vessel is 93.5m high and is equipped with two types of hydraulic impact hammers, namely YC40 and YC35. The "Yuehang 03" vessel is equipped with two types of diesel hammers, namely D160 and D138. The construction flow chart for the offshore rock socketed piles which are composed of steel pipe pile and cast-in-place pile for shallow-buried (exposed) rock layers is shown in Figure 2. To ensure that the steel pipe piles do not shift or even topple under the impact of ocean waves after being driven in, stabilization operations are required. The specific steps are as follows.

(1) Before the construction of the engineering pile, some auxiliary piles on the bank side should be constructed first (with sufficient penetration depth to stabilize them), and these auxiliary piles should be connected as a whole.

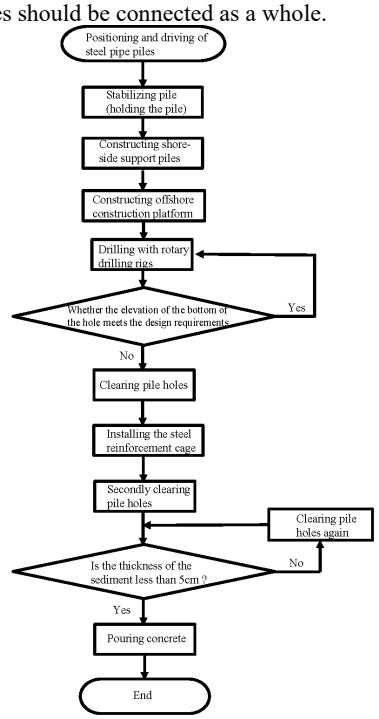

Figure 2. Flow chart of construction

(2) After the engineering pile (steel pipe pile) is driven, the pile should be temporarily fixed using the pile clamping frame of the driving vessel, and then connected with the nearby stable piles (welded with I-beams, i.e., clamped piles), as shown in Figure 3.

(3) Connect this engineering pile with the auxiliary piles on the bank side, and for piles in areas with shallow-buried rock layers or even exposed areas, additional auxiliary piles should

be placed around the engineering pile, and they should be connected with the bank-side auxiliary piles through the main beam to form a "bench" as the support piles for the construction platform. This structure is called the "bench effect".

Figure 3. Pile clamping

(4) Build the construction platform on the support piles, and complete the drilling of the engineering pile and the pouring of concrete.

(5) After the concrete of the engineering pile has hardened, use this pile as the support pile, continue to build the construction platform on the sea side, and complete the construction of all the engineering piles on the sea side using a similar method.

Additionally, during the pile driving process, it was found that for the granite stratum, when the penetration was not less than 30mm per strike, the toe of the steel pile did not crimp when the pile was driven. While when the penetration was less than 30mm per strike, the crimping sometimes occurred. In this project, the drilling of the cast-in-place piles was carried out using two types of rotary drilling machines, namely Xugong XR400E and XR360E, with maximum output powers of 373kW and 345kW respectively. During the rotary drilling process, by analyzing the characteristics of the rock samples obtained through drilling as shown in Figure 4.

Figure 4. Rock core of moderately weathered granite

It is possible to determine whether the bottom of the pile has reached the moderately weathered granite (Wang & Lou, 2023), thereby controlling the depth of the pile reaching the rock, and meeting the design requirement that the drilling should stop when the depth reaches 5 m or 10 m into the moderately weathered granite.

3.2 *Test Overview*

Preliminary theoretical calculations have revealed that the ultimate end-bearing resistance of the A3-21# test pile is greater than the ultimate shaft resistance, and there is no equilibrium point (i.e., the position where the ultimate shaft resistance and self-weight of the upper section of the pile balance with the ultimate shaft resistance and ultimate end-bearing resistance of the lower section of the pile). Therefore, the load cell should be installed at the bottom of the pile. If the upper section of the pile is pushed out during the test, additional counterweights can be added at the top of the pile to continue the test. However, considering that if the load cell is directly installed at the bottom of the pile, it is not conducive to the reverse flushing of the sediment at the bottom of the pile by the first batch of concrete during concrete pouring, which may affect the removal of sediment at the bottom of the pile. To ensure better load transmission between the load cell and the bearing stratum at the pile toe, the load cell will be installed at a position approximately 1 m from the bottom of the pile in this test, that is, at an elevation of -25.5 m.

The maximum unidirectional test load shall be calculated as following

$$Q_{nu} = \frac{\bar{\lambda} Q + W}{\bar{\lambda} + 1} \tag{1}$$

where, Q_{nu} is the maximum unidirectional test load of the load cell, kN. $\bar{\lambda}$ is the weighted tensile friction coefficient or friction coefficient of secondary type of compression owing to the pile shaft also bearing compression without tip constraints for the pile; Here the coeficient of secondary type compression is defined as the ratio between shaft side friction for the compression without tip constraint and with tip constrain. W is the sum of the self-weight and additional counterweight of the upper pile, kN. Q is the maximum test load of the static axial compression load test, kN. After calculation, the maximum unidirectional test load of this test is 3,493kN.

In order to obtain the shaft frictional resistance and the end resistance of the piles in each soil layer, vibrating wire rebar stress gauge sensors (referred to as rebar stress gauge, two of which were symmetrically installed for each test section) were installed at the interface of different soil layers and at different depths of the granite, as shown in Figure 1. The bottommost group of rebar stress gauges were close to the pile end to test the end resistance of the pile.

Based on Technical Specification for Testing and Inspection of Port and Waterway Engineering Foundation Pile (JTS 240-2020) (MTPRC, 2020), the ultimate axial compressive bearing capacity of pile is determined as follows:

$$Q_{\mathrm{u}} = \frac{Q_{\mathrm{uu}} - W}{\bar{\lambda}} + Q_{\mathrm{ud}} \tag{2}$$

where, Q_{u} is the ultimate axial compressive bearing capacity of pile, kN. Q_{uu} is the ultimate loading value of the upper section of the pile, kN. Q_{ud} is the ultimate loadning value of the lower section of the pile, kN.

4 EXPEREMENTAL RESULTS AND ANALYSIS

4.1 *Displacements of top panel and bottom panel of load cell and pile top at different loading stage*

The test process was carried out in accordance with the specification (MTPRC, 2020). The load-displacement curves (Q-s) of the A3-21# test pile under different loads are shown in Figure 5. It can be found from Figure 5 that:

(1) At the maximum unidirectional test load of 3,493kN, the displacements of the top panel, bottom panel and pile top were 1.58 mm, 3.51 mm and 0.5 mm respectively. After all loads were removed, the residual displacements of the top panel, bottom panel and pile top are 0.18 mm, 0.83 mm and 0.12 mm respectively. According to specification (MTPRC, 2020), the ultimate bearing capacity of the upper section and lower section of the pile were not less than the maximum test load. According to Eq.(2), the ultimate axial compressive

bearing capacity of the A3-21# test pile was not less than 7,000 kN.

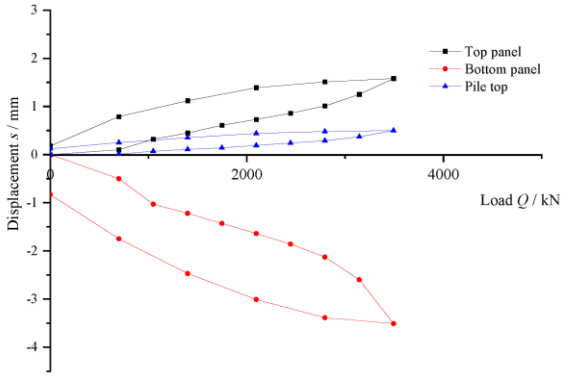

Figure 5. *Q-s* curves of test pile A3-21#.

(2) Under the maximum test load, the displacements of the upper and lower sections of the pile were very small, much less than 40 mm, which indicates that the design of this pile was very conservative.

(3) Although the load cell was installed close to the pile bottom, the displacement of the bottom panel was greater than that of the top panel, and the displacement of the bottom panel occurs earlier than that of the top panel. The reasons are mainly in three aspects. First, when calculating the equilibrium point, the shaft friction resistance and end resistance of the granite are taken as the values based on the experience of other similar geological projects, but the actual granite parameters of this project and these values are quite different, and the geology of the test pile may have deviated from the geological drilling hole as shown in Figure 1, which led to inaccurate calculation of the equilibrium point. Second, there is a slight sediment at the bottom of the cast-in-place pile, which led to a reduction in the pile end bearing capacity. And third, the tensile friction coefficient (friction coefficient of secondary type compression) used for calculating the equilibrium point had a certain error compared with the actual situation, resulting in a deviation in the calculation results.

(4) Before the load reached 2,794.4 kN, the *Q-s* curves basically showed a linear relationship. However, after reaching 2,794.4 kN, the slope of the *Q-s* curves became significantly larger compared to that for previous test load.

(5) It shows that the work as jet force Q times displacement s is quite different between at top panel and bottom panel. The magnitude of Q times s is larger at bottom panel. While the slope of $\Delta Q/\Delta s$ at each increase of force is larger for top panel than for bottom panel, this means the total stiffness of the pile-soil system is larger for the top section. When decreasing the jet force, it can be discovered that more plastic deformation generated at the bottom section of pile.

4.2 *Axial force of test pile under different loads*

According to the calibration certificate of rebar stress gauge, the stress and strain of rebar stress gauge are calculated using the following equations:

$$\Delta\varepsilon = K_0(f^2 - f_0^2) \quad (3)$$

$$\sigma_s = K\Delta\varepsilon \quad (4)$$

$$\varepsilon_s = \frac{\sigma_s}{E_s} \quad (5)$$

where, $\Delta\varepsilon$ is the frequency value, με. f is the measured frequency, Hz. f_0 is the zero-point frequency, Hz. K_0=0.00071186. K is the calibration coefficient. E_s is the elastic modulus of the rebar stress gauge, MPa. σ_s is the stress of the rebar stress gauge, MPa. ε_s is the strain of the rebar stress gauge.

Considering the deformation compatibility condition, the strain of the pile shaft is the same as the strain of the rebar stress gauge at the same cross section. Therefore, the axial force of the pile can be calculated by the following formula:

$$F = E\varepsilon_s A \quad (6)$$

where, F is the axial force of the pile, kN. E is the elastic modulus of the pile, kPa. A is the cross-sectional area of the pile, m².

By combining Eqs (3) to (6), the axial force distribution diagram and strain diagram of the A3-21# test pile shaft are shown in Figures 6 and 7 respectively. From Figure 6, it can be seen that the axial force of the pile shaft increases with the increase of the test load, and at the maximum test load, the axial force of the bottommost test section of the pile shaft is 2,423.34 kN, which means that the pile end resistance is 2,423.34 kN. Meanwhile, the load gradually acts from the load cell to the top and bottom of the test pile, and is mainly beared by the moderately weathered granite with an elevation from -20.17 m to -26.17 m.

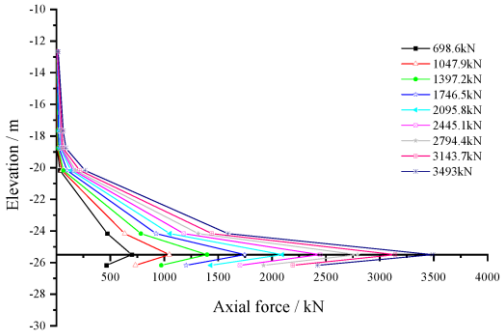

Figure 6. Axial force distribution of test pile under different loads

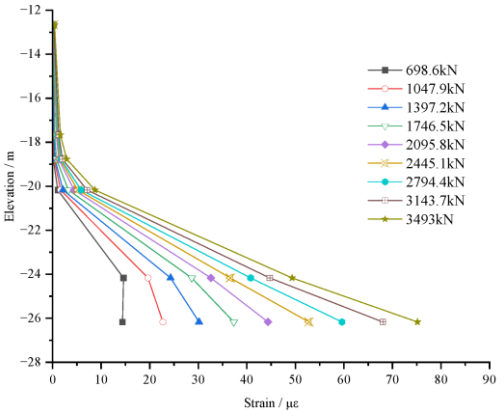

Figure 7. Strain diagram of test pile under different loads

Figure 7 shows that strains varies with locations and magnitude of loading. In general, each strain increased with increase in load at each position. Below the load cell, the compression strain is the largest along the depth at any magnitude of load, excluding at the first loading process at 698.6 kN. Notable compression strain below the load cell is reasonable owing to its resistance of combined force from loading jet and gravitional weight of the pile above load cell. Of course, at the lower loading force of 698.6 kN, the strain exactly above the load cell, seeing elevation about -24.0 m, is larger than that below the load cell, it might be a relative broken rock providing reaction force intially. The compression strain cloase and above elevation -21.0 m is relative small, this means that the reaction force is mainly provided at moderately

weathered granier under self-balance loading condition. It is found that above -18.0 m, which the pile body is composed of steel pipe and inner reinforced conceret pile, the strain is small that less axial force generated to react the bottom lifting force.

4.3 *Friction and pile-soil relative displacement relationship*

The friction between two adjacent test cross-sections *i* and *i*+1 of the test pile shaft is calculated by the following formula:

$$q_{si} = \frac{|F_i - F_{i+1}|}{u \cdot l_i} \quad (7)$$

where, q_{si} is the friction between test cross-sections *i* and *i*+1 of the test pile shaft, kPa. F_i is the axial force of the pile shaft at test cross-section *i*, kN. F_{i+1} is the axial force of the pile shaft at test-cross section *i*+1, kN. l_i is the distance between test-sections *i* and *i*+1, m. *u* is the perimeter of the pile cross-section , m; F_i and F_{i+1} are calculated using Eq. (6).

According to Eq (7), the test values of the soil resistance on the side of the A3-21# test pile under the maximum unidirectional test load of 3,493 kN can be obtained, as shown in Table 3.

Table 3. Test value of soil resistance on side of pile

Soil layer number and name	Elevation range（m）	Test value of soil resistance on side of pile（kPa）	Remark
③$_2$、③$_{2\text{-}1}$ Silty clay	-12.67 ~ -17.67	3.0	Upper section pile. Steel pile
⑤ Granite residual soil	-17.67 ~ -18.77	7.21	Upper section pile. Steel pile and cast-in-place pile
○, 9$_{2\text{-}2}$ Fragmented, strongly weathered granite	-18.77 ~ -20.17	40.03	Upper section pile. Cast-in-place pile
	-20.17 ~ -24.17	105.55	Upper section pile. Cast-in-place pile
○, 9$_3$ Moderately weathered granite	-24.17 ~ -25.50	455.01	Upper section pile. Cast-in-place pile
	-25.50 ~ -26.17	509.36	Lower section pile. Cast-in-place pile

It can be found in Table 3 as the follows.

The tensile (secondary type compression) side friction resistance and compression side friction resistance of cast-in-place pile at moderately weathered granite are not less than 455.01 kPa and 509.36 kPa respectively. For the fragmented, strongly weathered granite, the tensile (secondary type compression) side friction resistance of cast-in-place pile is not less than 40.03 kPa. This value is small because the corresponding test sections are far from the load cell, and the soil resistance on the side of the pile has not been fully excited. These values 455.01kPa and 509.36kPa can be used to compensates for the lack of rock parameters of the geological survey report that not provided tensile (secondary type compression) side friction resistance and compression side friction resistance of cast-in-place pile at moderately weathered granite, and be used for the verification of the bearing capacity of the pile foundation and the optimization of the pile length.

The tensile (seconary type compression) coefficient of cast-in-place pile at moderately weathered granite (that is, the ratio of tensile (secondary type compression) side friction resistance to compression side friction resistance) is approximately 0.9.

According to Design Code for Wharf Structures (JTS 167-2018) (MTPRC, 2018) and Table 2, and considering that the friction resistance of pile shaft at the moderately weathered granite is not less than 509.36kPa based on the test result, the theoretical calculated value of the ultimate axial compressive bearing capacity of test pile A3-21# is not less than 19,983 kN. Compared with the designed ultimate axial compressive bearing capacity of 7,000 kN, it has a surplus of no less than 185%, which means that the bearing capacity of this pile is rather conservative and there is a significant space for optimizing the pile length.

The pile-soil relative displacement is calculated by the following equation

$$\delta_i = s - L_1\varepsilon_1 - \sum_{j=2}^{i} \frac{L_j}{2}(\varepsilon_j + \varepsilon_{j+1}) \quad (8)$$

where, δ_i is the pile-soil relative displacement of the i-th (where $i \geqslant 1$) segment of the upper (lower) section pile, measured from the top (bottom) panel of the load cell. L_1 is the length from the test cross-section closest to the load cell in the upper (lower) section of the pile to the top (bottom) panel of the load cell. L_j is the length of the *j*-th pile segment. *s* is the displacement of the top (bottom) panel of the load cell. ε_1 is the strain of the rebar stress gauge at the test cross-section closest to the top (bottom) panel in the upper (lower) section pile. ε_j and ε_{j+1} are the strain of rebar stress gauge at the *j*-th and (*j*+1)-th test cross-sections from the top (bottom) panel of load cell in the upper (lower) section pile.

In order to further reveal the mechanism of the frictional resistance of the A3-21# test pile, the pile-soil relative displacement between different positions of rebar stress gauge installing can be calculated according to Eq. (8). The curves of the pile-soil relative displacement and the side frictional resistance under different loads at the moderately weathered granite area are shown in Figure 8. Figure 8 shows that when the pile-soil relative displacement at the moderately weathered granite area is less than 2.09 mm, the side frictional resistance of the pile and the pile-soil relative displacement basically shows a linear relationship. At the maximum test load, the pile-soil relative displacement at the moderately weathered granite is 3.46 mm. At this point, the side friction resistance of the pile has not been fully exerted. If the load was increased, a greater side friction resistance of the pile could be obtained.

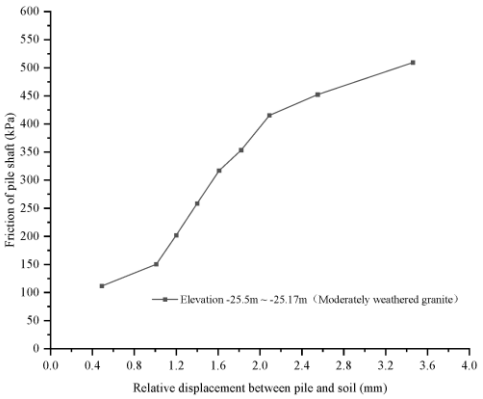

Figure 8. The relationship curve of pile-soil relative displacement and friction of test pile.

5 CONCLUSIONS

Through the technique research on the pile driving, drilling, pouring and mechanical test study on a rock socketed pile using self-balancing test in the Phase I Project of the East Port Area of Yantian Port, some technical parameters are obtained and the main conclusions are drawn as follows.

(1) For the construction of the offshore rock socketed piles which are composed of steel pipe pile and cast-in-place pile in shallow-buried (or exposed) granite strata with strong waves and strong winds, certain numbers of auxiliary piles can be placed around the steel pile, and these auxiliary piles are connected with the steel pile through the main beam to form a "bench", and the drilling and concrete pouring inside the pile can be successfully completed.

(2) In the granite strata of Yantian Port, when the penetration is not less than 30 mm/stroke, the toe of the steel pile does not crimp during driving.

(3) A self-balance test method for a composite steel pipe with reinforced cast-in-place pile was established. The self-balancing test shows that The side friction resistance per unit area of cast-in-place pile at moderately weathered granite is not less than 509.36 kPa, and the tensile side friction coefficient (or friction coefficent of secondary type compression) is approximately 0.9. When the pile-soil relative displacement at the moderately weathered granite area is less than 2.09 mm, the side frictional resistance of the pile and the pile-soil relative displacement basically shows a linear relationship.

(4) the bearing capacity of pile on the theoretical basis was evaluated, and the theoretical value of the ultimate axial compressive bearing capacity of the test pile is not less than 19,983 kN, and has a surplus of no less than 185% compared with the designed ultimate bearing capacity of 7,000 kN.

6 REFERENCES

Chen, S. C., 1999. Construction Technology of Underwater Rock-socketed Cast-in-situ Piles. *Chian Harbor Engineering.* 5: 41-46.

Hu, L. W., 2006. Mechanical Test Study on Fully Grouted Bolts Applied in Yantian Port. *Ground Modification and Seismic Mitigation* (ASCE), GSP 152: 193-198.

Lou, X. Q., Wang, X., Lv, S. H., Wang, Z. 2018. Analysis on uplift and compression resistance of cast-in-situ piles in soft rock area. *Port & Waterway Engineering.* 5: 165-170, 182.

Xue, Z. N., Tian, Y. Q., Dong, Y. Q., Zhou, Z. J. 2022. Study on Value of Lateral Friction Resistance of Bored Cast-in-situ Pile in Loess Area Considering Influence of Length-diameter Ratio. *Journal of Highway and Transportation Research and Development*, 39(12): 67-74, 85.

Zhang, Y. T., Liu, Y. Q., Chen, P. S., Luo, H. W., Deng, Z. Q., Yu, C. C. 2023. Research and application of lateral friction resistance characteristics and coefficient value of cast-in-place piles in coral reef limestone strata. *Chinese Journal of Rock Mechanics and Engineering*, 42(3): 748-757.

Wu, R. H., Ye, J. F., Luo, G. J., Shen, X. L., Zhang, Q. 2021. Experimental study on the bearing characteristics of steel pipe pile in radial sandbar of Jiangsu province. *The Ocean Engineering*, 39(1): 121-132.

Wu, H., Hu, X. H., Zhao, L. Q., Lou, X. Q. 2023. Experiment on pile sinking and bearing characteristics of steel pipe piles in dense gravel soil bearing stratum at sea. *Port & Waterway Engineering*, 7: 212-217.

Xu, X. Y., Lv, H., Yao, S. 2012. Experimental study on axial loading-bearing characteristics of large-diameter steel-pipe pile on deep sediment layer. *Port & Waterway Engineering*, 6: 179-182.

Han, G. X., Qian, Z. C., 2023. Research on the accumulation characteristics of pile side friction resistance on soil interface of large diameter cast-in-situ piles. *Hydro-Science and Engineering*, 6:161-167.

Hu, L. W., Lou, X. Q., Zhou, M., Xu, W. Q. 2023.Static load study on in-situ steel pipe pile for offshore wind farm using self-balancing method. *The Ocean Engineering*, 41(1):141-151.

Wang, Q. Y., Lou, X. Q. 2021. Construction technology of bored cast-in-place piles in coral reef stratum. *Engineering Technology*. 10:295-301.

Ministry of Transport of the People's Republic of China (MTPRC). 2020. Technical Specification for Testing and Inspection of Port and Waterway Engineering Foundation Pile: JTS 240-2020. Beijing: People's Communications Press Co., Ltd.

Ministry of Transport of the People's Republic of China (MTPRC). 2018. Design Code for Wharf Structures: JTS 167-2018. Beijing: People's Communications Press Co., Ltd.